Supporting Information

Palladium / Cobalt Nanowires with Improved Hydrogen Sensing Stability at Ultra-Low Temperatures

Lingling Du, [1] Dongliang Feng, [1] Xiaxia Xing, [1] Yang Fu, [1] Luis F Fonseca [2] and Dachi Yang [1] *

[1]Department of Electronics, College of Electronic Information and Optical Engineering, Nankai University, Tianjin 300350, China

*E-mail: yangdachi@nankai.edu.cn

[2] Department of Physics, University of Puerto Rico Rio Piedras, San Juan, PR 00931, USA

Contents

Figure S6. The hydrogen-sensing response of $Pd_{82}Co_{18}$ NWs sensor at (a) 243 K, (b) 210 K, (c)180 K, respectively.

Figure S7. The hydrogen-sensing response of $Pd_{63}Co_{37}$ NWs sensor at (a) 243 K, (b) 210 K, (c)180 K, (d) 150 K, respectively.

Figure S8. The hydrogen-sensing response of $Pd_{33}Co_{67}$ NWs sensor at (a) 243 K, (b) 180 K, respectively.

Figure S9. The selective response of $Pd_{63}Co_{37}$ NWs sensors toward 2% H_2 and interfering gases, including 2% NH_3, CO, H_2S and 0.5% NO at room temperature.

Figure S10. The hydrogen-sensing performance of pure Co NWs sensor at (a) 273 K, (b) 298 K, (c) 358 K, respectively.

Figure S11. The transient response curves of the $Pd_{82}Co_{18}$ NWs sensor towards various H_2 concentrations under various temperatures.

Figure S12. The transient response curves of the $Pd_{63}Co_{37}$ NWs sensor towards various H_2 concentrations under various temperatures.

Figure S13. The transient response curves of the $Pd_{33}Co_{67}$ NWs sensor towards various H_2 concentrations under various temperatures.

Experimental section

Preparation of PdCo NWs

The optimized PdCo NWs were prepared though the AAO-confined electrodeposition method similar to previous publications.[1-3] Specifically, the samples with various chemical content of palladium/cobalt were prepared by regulating the molar ratio of $PdCl_2$ (Palladium chloride, AR, Pd content > 59.5 wt%, CAS: 7647-10-1, Mascot) and $CoSO_4 \cdot 7H_2O$ (Cobalt sulfate, AR, ≥ 99%, CAS:10026-24-1, Aladdin) in electrolytic solution. In addition, the electrolytes also contained 0.2 g/L $C_{12}H_{25}SO_4Na$ (AR, ≥ 99.5%, CAS: 151-21-3, Huawei Ruike) and 0.08 M H_3BO_3 (GR, ≥ 99.5%, CAS: 10043-35-3, Xiya Reagent), followed by being buffered to pH ≈ 8 with $NH_3 \cdot H_2O$ (ACS, 28.0-30.0% NH_3 basis, CAS: 1336-21-6, Aladdin).

The preparation of AAO template utilizes similar procedures to previous publications. [4] Before electrodeposition, one side of the AAO templates was covered with a sputtered thick Au layer to guarantee the covering of the AAO pores. [4] Then, the electrodeposition was conducted with two-electrode systems using a graphite plate as the counter electrode, and the gold/AAO templates as the working electrode. The PdCo NWs grow along with the nanochannels in the AAO templates under a constant voltage of 1.8-2.3 V and at room temperature. 4 M NaOH (ACS, ≥ 97%, CAS: 1310-73-2, Aladdin) served as the etching solution to remove the AAO templates at 60 ^oC for 150 min. The PdCo NWs were rinsed thoroughly in deionized water and dried at 50 ^oC.

Characterization

Field-emission scanning electron microscopy (FE-SEM, JEOL-6701F) was performed

to obtain the images of the samples. Transmission electron microscopy (TEM, JEOL-2010) with high resolution TEM (HRTEM, JEOL-2010) was conducted for the high-resolution image. The elemental mappings were obtained with energy dispersive X-ray spectroscopy (EDX) and the atomic ratio was used as the reference to the samples. X-ray diffraction (XRD) with Cu Kα (λ = 1.5406 Å), and X-ray photoelectron spectroscopy (XPS, Thermo Scientific ESCALAB 250Xi) were carried out to characterize the crystallographic information and the chemical composition of the samples, respectively.

Building art of sensor prototypes and sensing evaluations

For the hydrogen sensing evaluation, the sensors prototypes were firstly built by integrating PdCo NWs in alcohol to the interdigital electrodes (IEDs), and dried at 50^{o}C in vacuum. Then, the prepared PdCo NWs sensor was mounted in a sealed chamber with gas inlets and outlets. Hydrogen sensing tests were performed with a test system similar to the one used in previous study. [3] Liquid nitrogen was used to cool the chamber to create the low-temperature test background. A temperature controller driven by external power sources was set below the sensing platform to maintain a constant temperature within the operating temperatures range of 150 K - 388 K. During testing, the various H_2 (99.99%, Air Liquide (Tianjin) co. LTD) concentrations (0.1% - 3%) balanced with high-purity Ar gas (99.99%, Air Liquide (Tianjin) co. LTD) were passed through the sample chamber, controlled by mass flow controllers (MFCs). A data collector (KEITHLEY, 2450 model) was used to set the applied voltage and show electric signals.

The hydrogen response of these sensors was normalized and defined as the ratio ($\Delta R/R_0$ (%)) of the electrical resistance variation (ΔR) and the baseline resistance (R_0). The resistance variation $\Delta R = R_g - R_0$, where R_0 and R_g are the real-time peak resistance value in background Ar gas and H_2 at different concentrations, respectively. The response / recovery time is defined as the time taken by the sensor to reach 90% of maximum resistance variation after turning on / off the hydrogen flux.

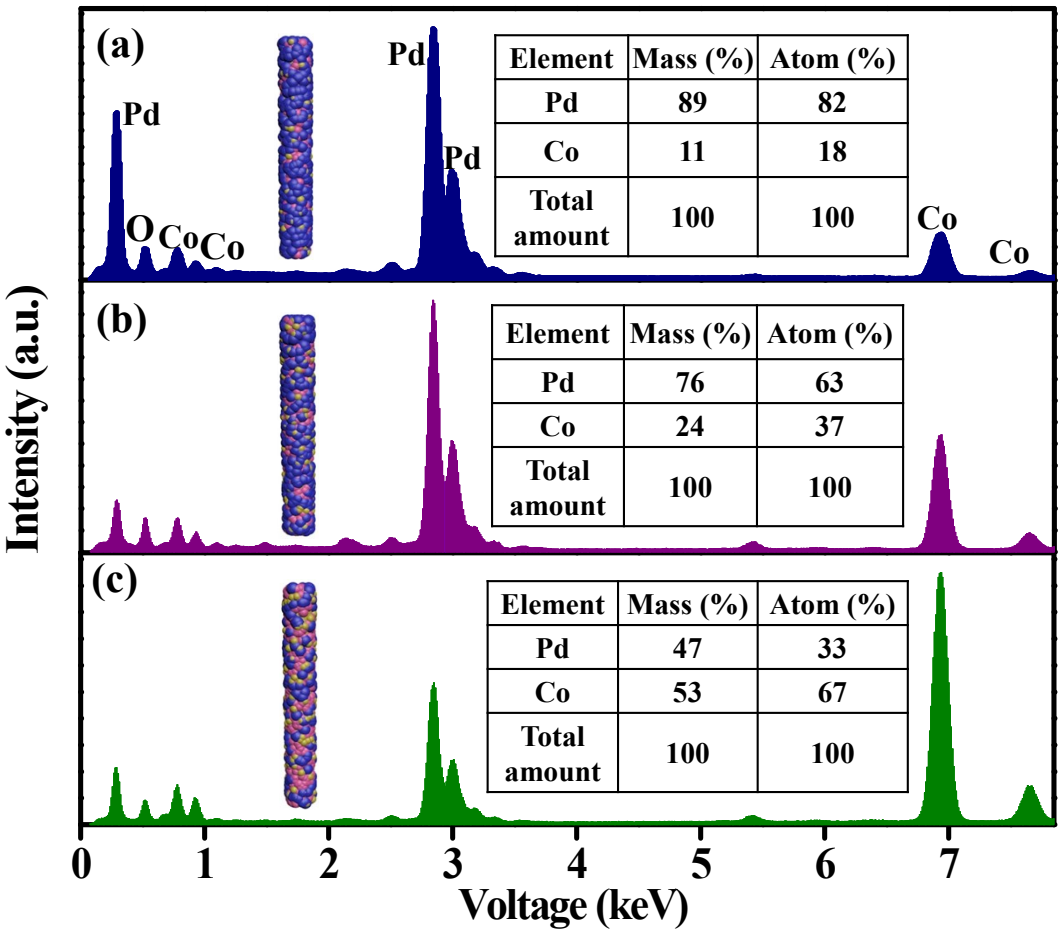

Figure S1. EDS analysis of PdCo NWs with various cobalt atomic ratios for (a) $Pd_{82}Co_{18}$, (b) $Pd_{63}Co_{37}$ and (c) $Pd_{33}Co_{67}$, respectively.

Table S1. Crystallite sizes calculated from XRD data by Scherrer formula.

Samples	Crystallite size (nm)
$Pd_{82}Co_{18}$	6.24
$Pd_{63}Co_{37}$	6.38
$Pd_{33}Co_{67}$	7.01

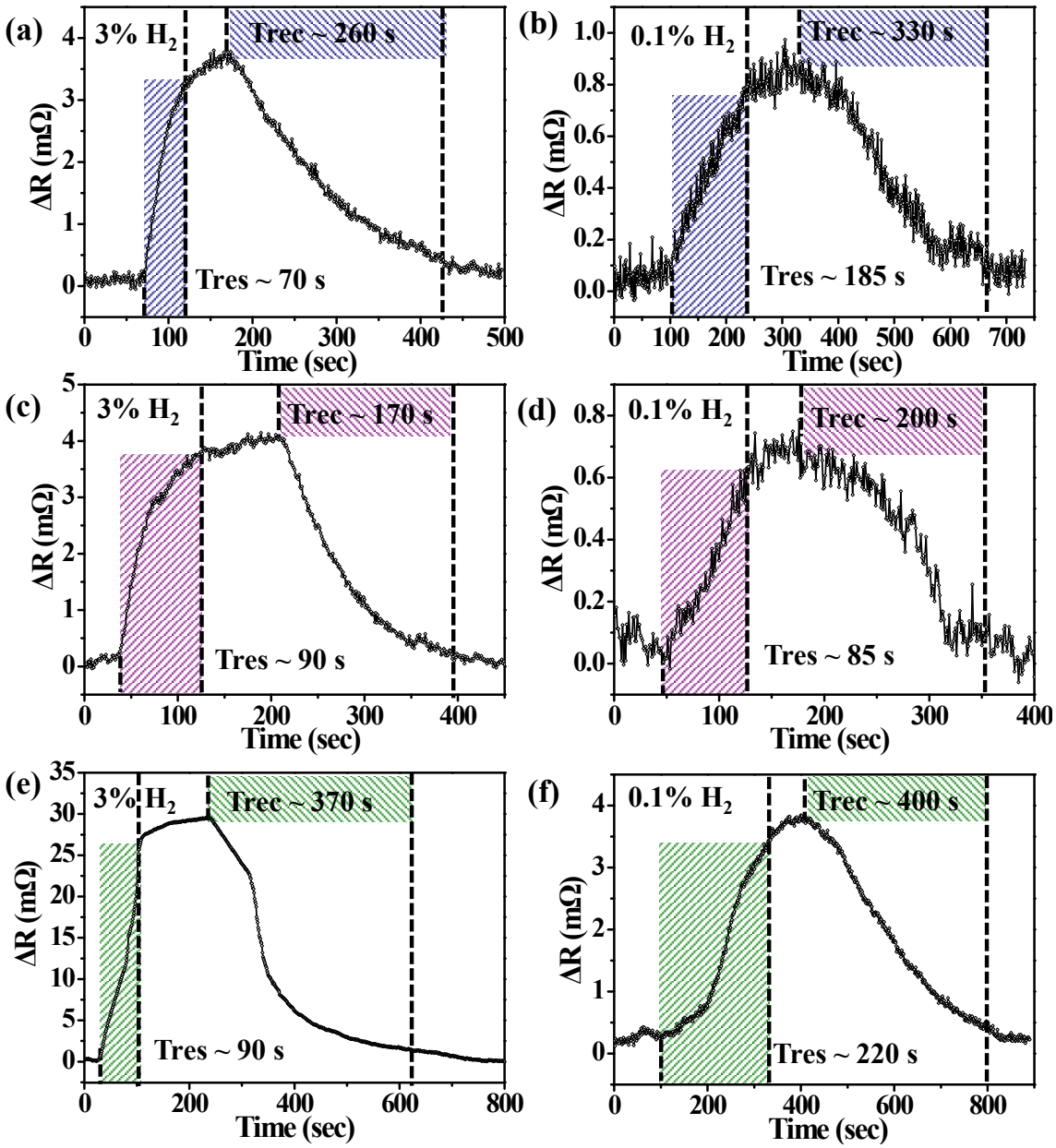

Figure S2. The response and recovery times toward 3% and 0.1% H_2 of (a) - (b) $Pd_{82}Co_{18}$, (c) - (d) $Pd_{63}Co_{37}$ and (e) - (f) $Pd_{33}Co_{67}$ at 273 K, respectively.

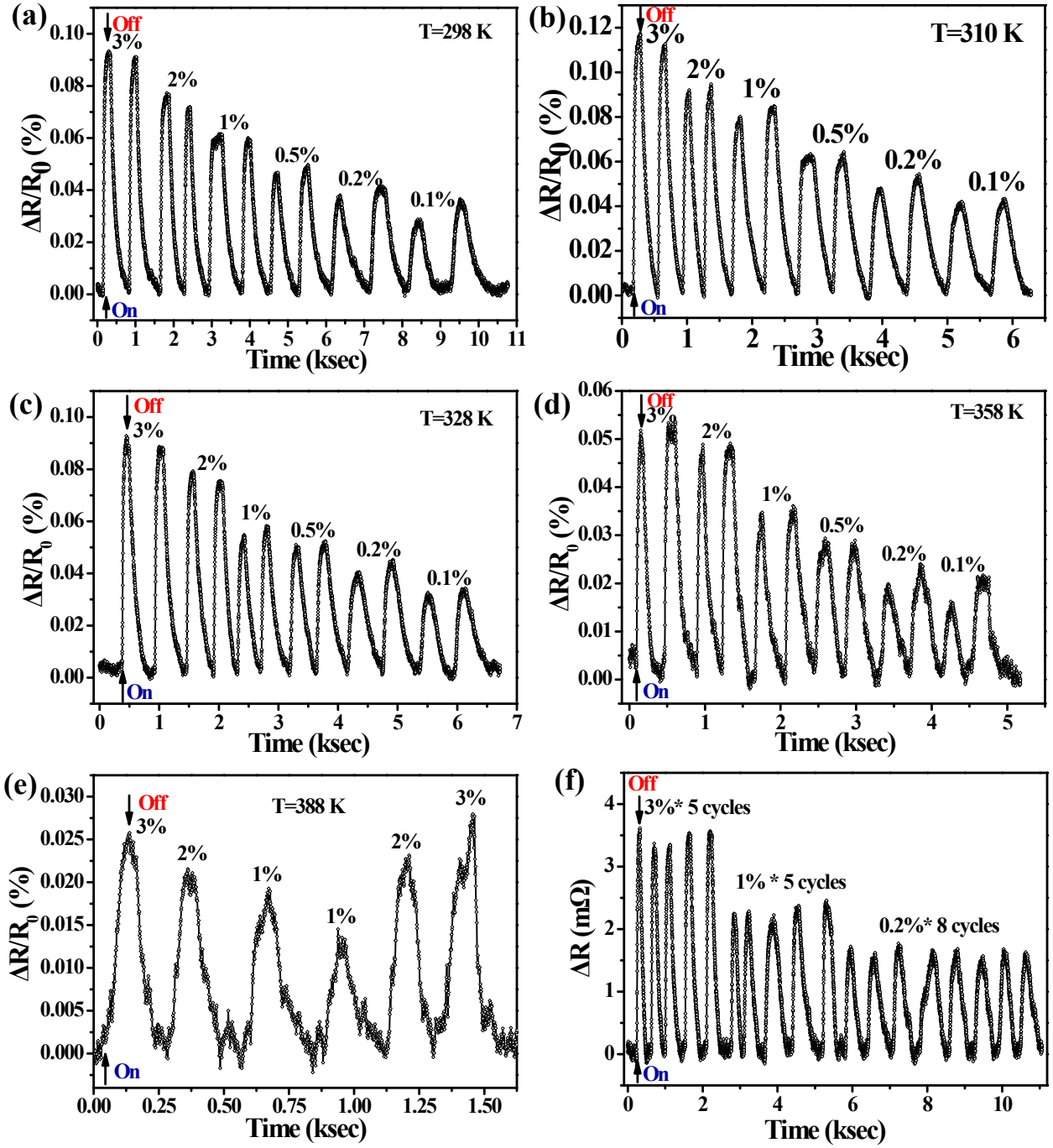

Figure S3. The sensing response to 0.1% - 3% H_2 of $Pd_{82}Co_{18}$ NWs sensor at (a) 298 K, (b) 310 K, (c) 328 K, (d) 358 K and (e) 388 K, respectively. (f) The repeatability of the sensor at room temperature.

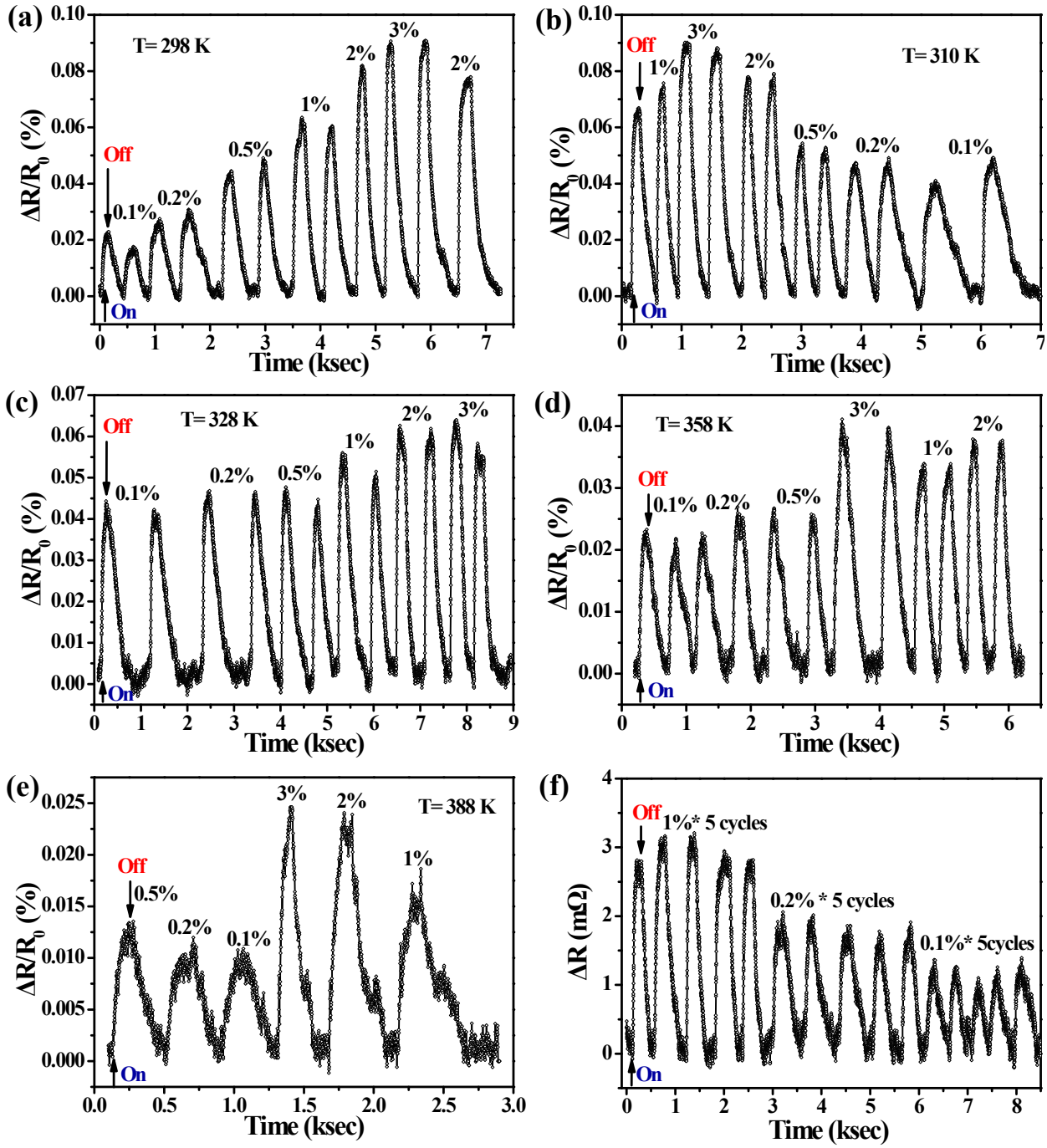

Figure S4. The sensing response to 0.1% - 3% H_2 of $Pd_{63}Co_{37}$ NWs sensor at (a) 298 K, (b) 310 K, (c) 328 K, (d) 358 K and (e) 388 K, respectively. (f) The repeatability of the sensor at room temperature.

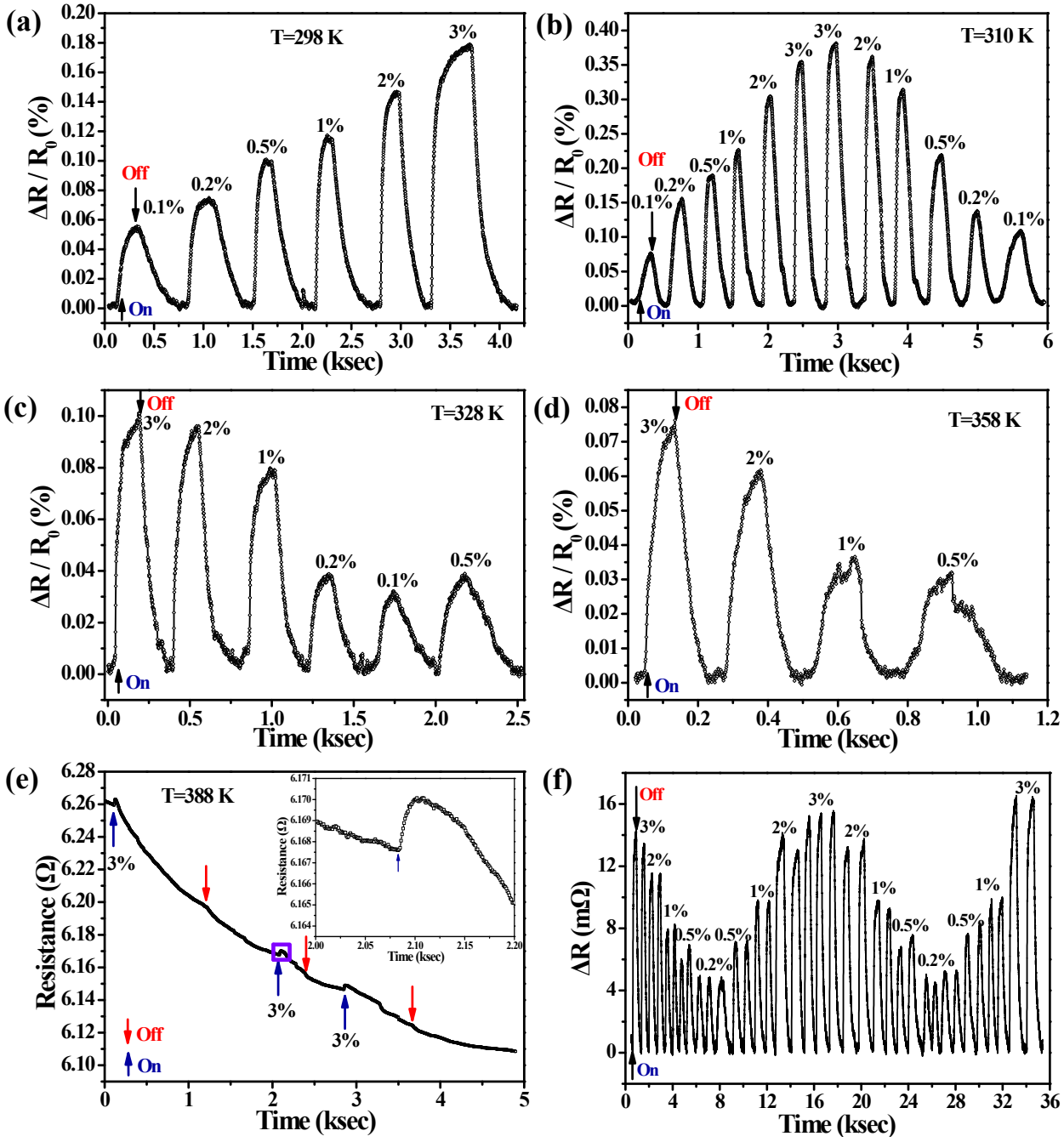

Figure S5. The sensing response to 0.1% - 3% H_2 of $Pd_{33}Co_{67}$ NWs sensor at (a) 298 K, (b) 310 K, (c) 328 K, (d) 358 K and (e) 388 K, respectively. (f) The repeatability of the sensor at room temperature.

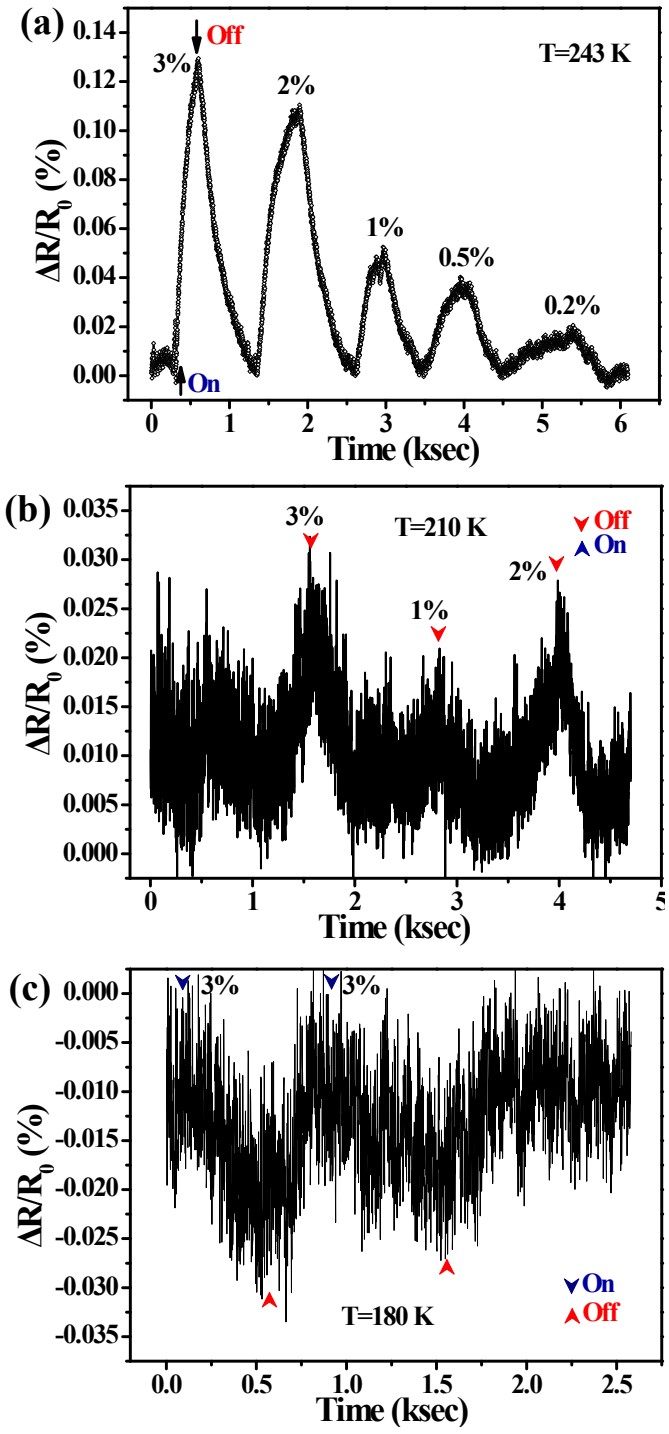

Figure S6. The hydrogen-sensing response of $Pd_{82}Co_{18}$ NWs sensor at (a) 243 K, (b) 210 K and (c) 180, respectively.

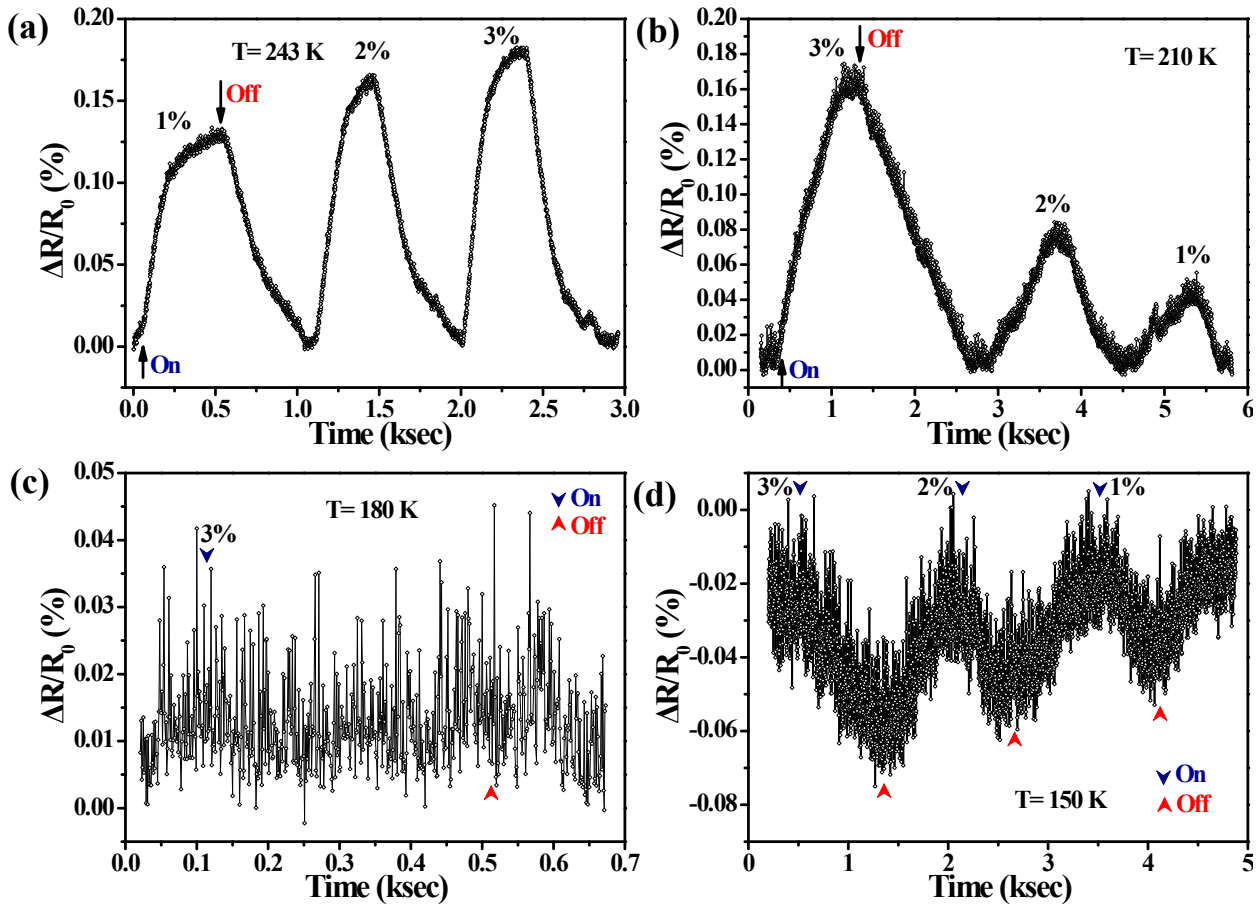

Figure S7. The hydrogen-sensing response of $Pd_{63}Co_{37}$ NWs sensor at (a) 143 K, (b) 210 K, (c) 180 K and (d) 150 K, respectively.

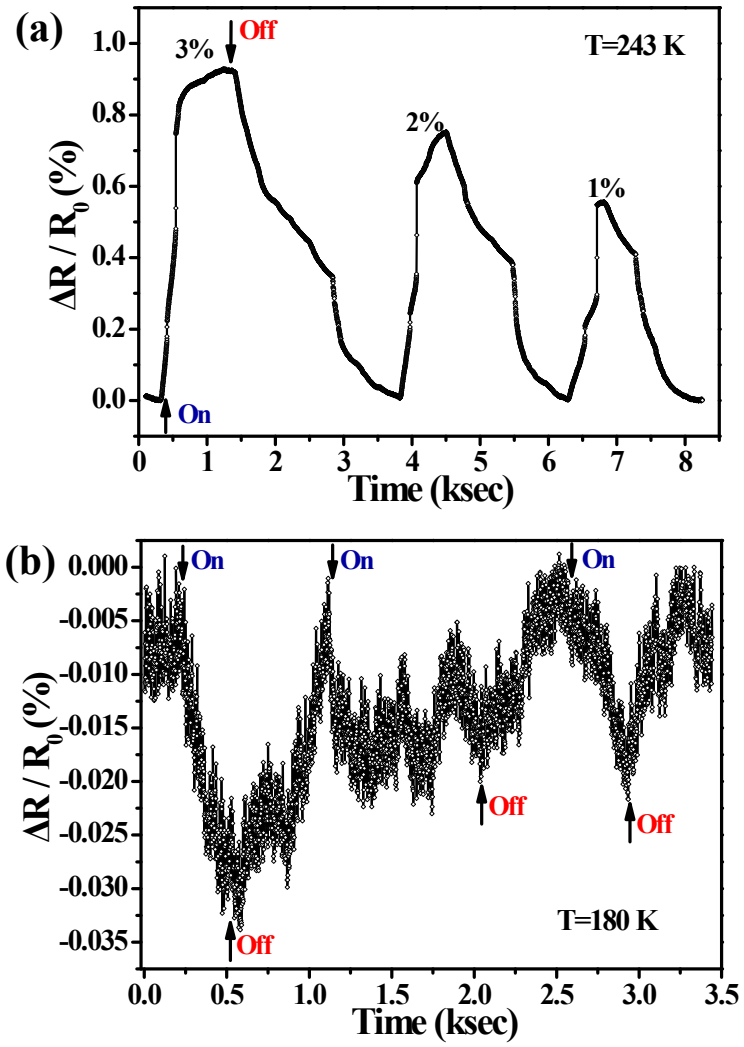

Figure S8. The hydrogen-sensing response of $Pd_{33}Co_{67}$ NWs sensor at (a) 243 K, (b) 180 K, respectively.

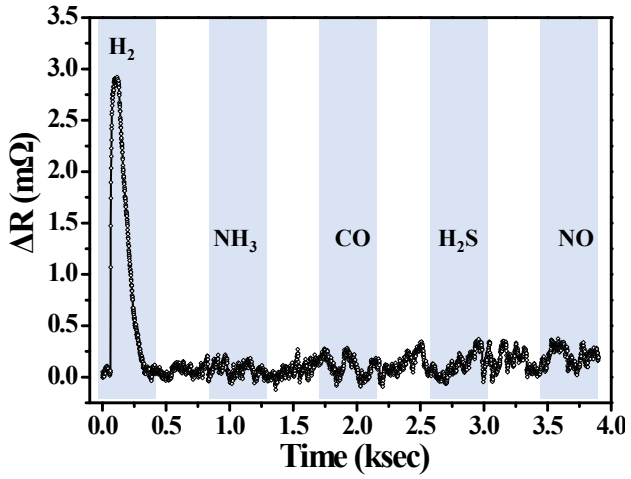

Figure S9. The selective response of $Pd_{63}Co_{37}$ NWs sensors toward 2% H_2 and interfering gases, including 2% NH_3, CO, H_2S and 0.5% NO at room temperature.

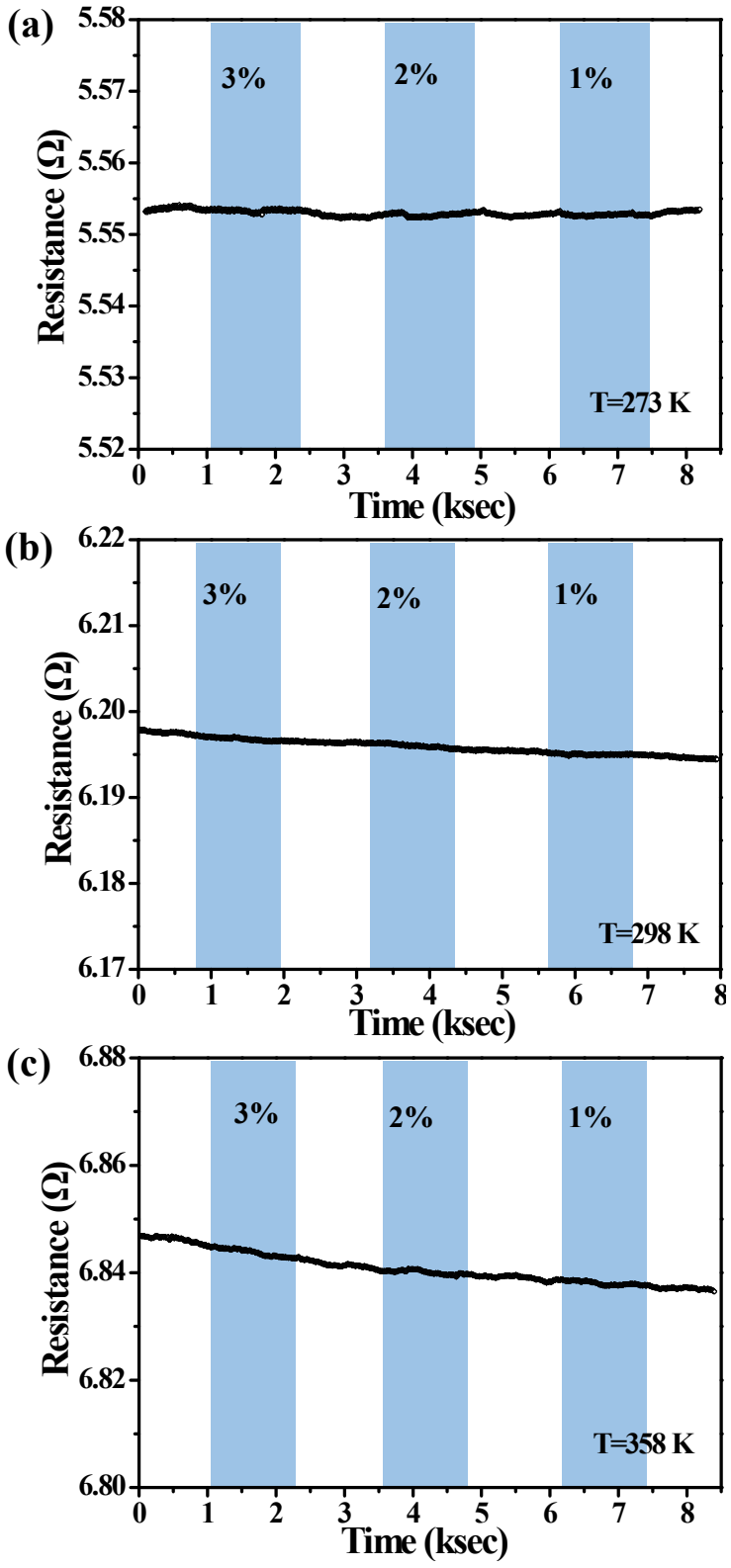

Figure S10. The hydrogen-sensing performance of pure Co NWs sensor at (a) 273 K, (b) 298 K, (c) 358 K, respectively.

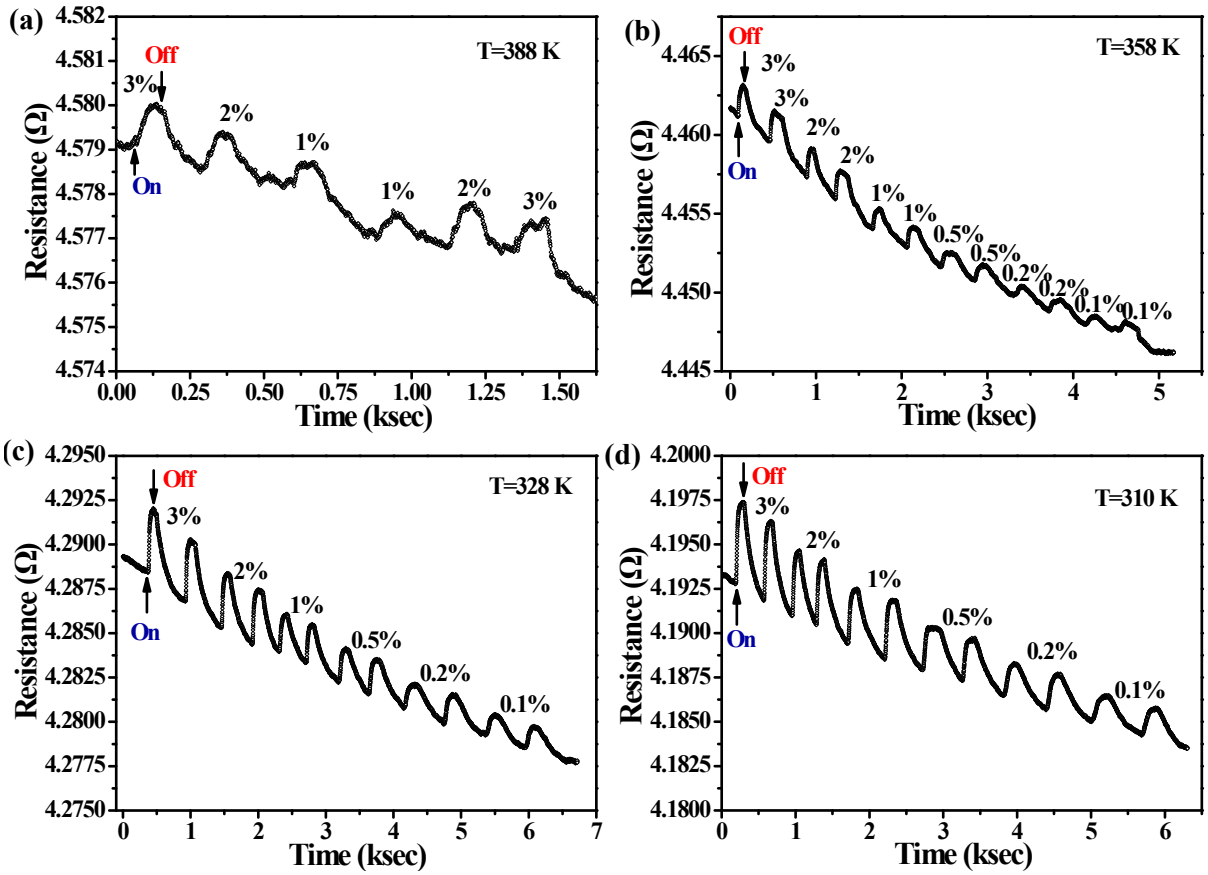

Figure S11-1. The transient response curves of the $Pd_{82}Co_{18}$ NWs sensor towards various H_2 concentrations at (a) 388 K, (b) 358 K, (c) 328 K and (d) 310 K, respectively.

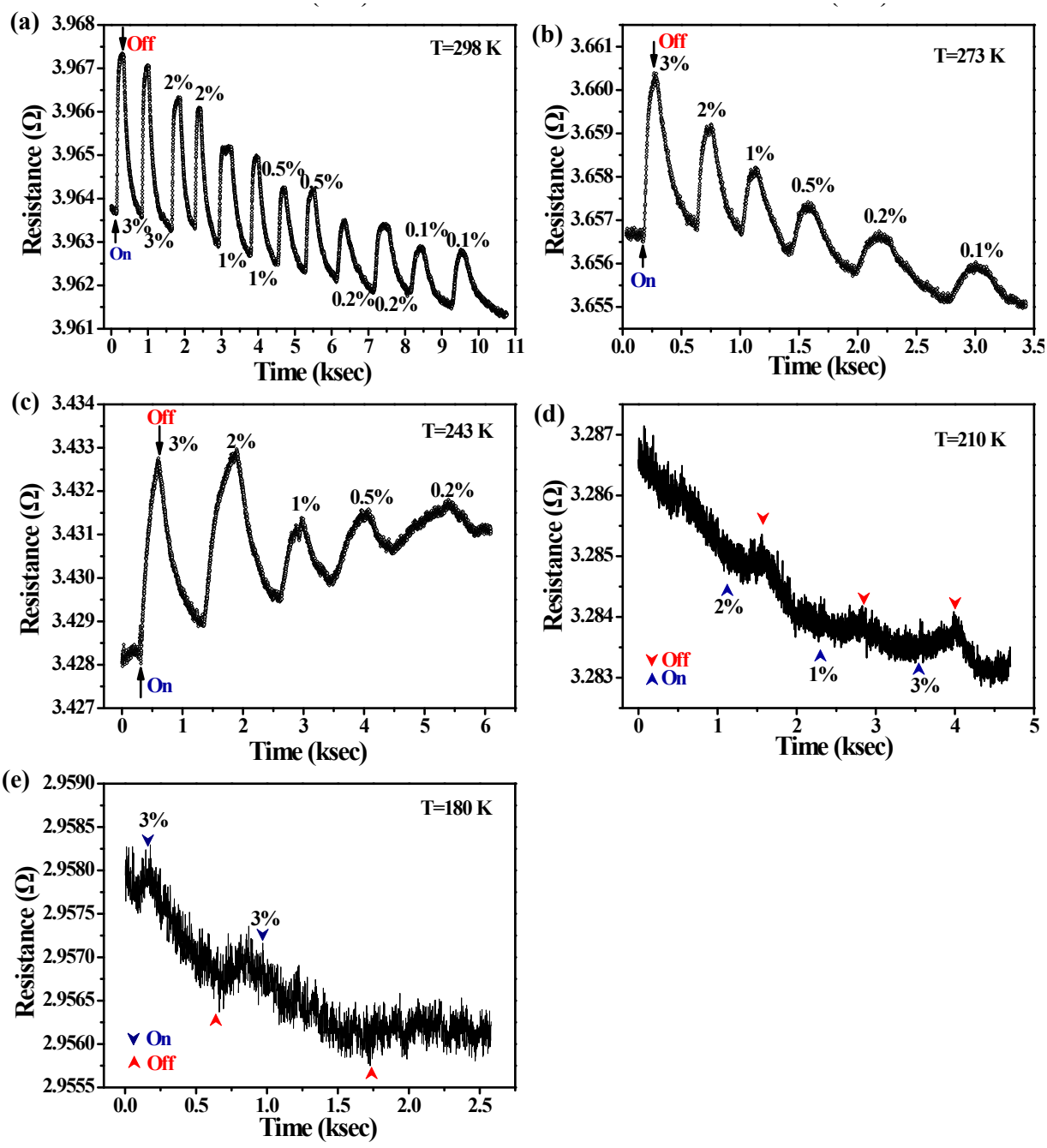

S11-2. The transient response curves of the $Pd_{82}Co_{18}$ NWs sensor towards various H_2 concentrations at (a) 298 K, (b) 273 K, (c) 243 K, (d) 210 K and (e) 180 K, respectively.

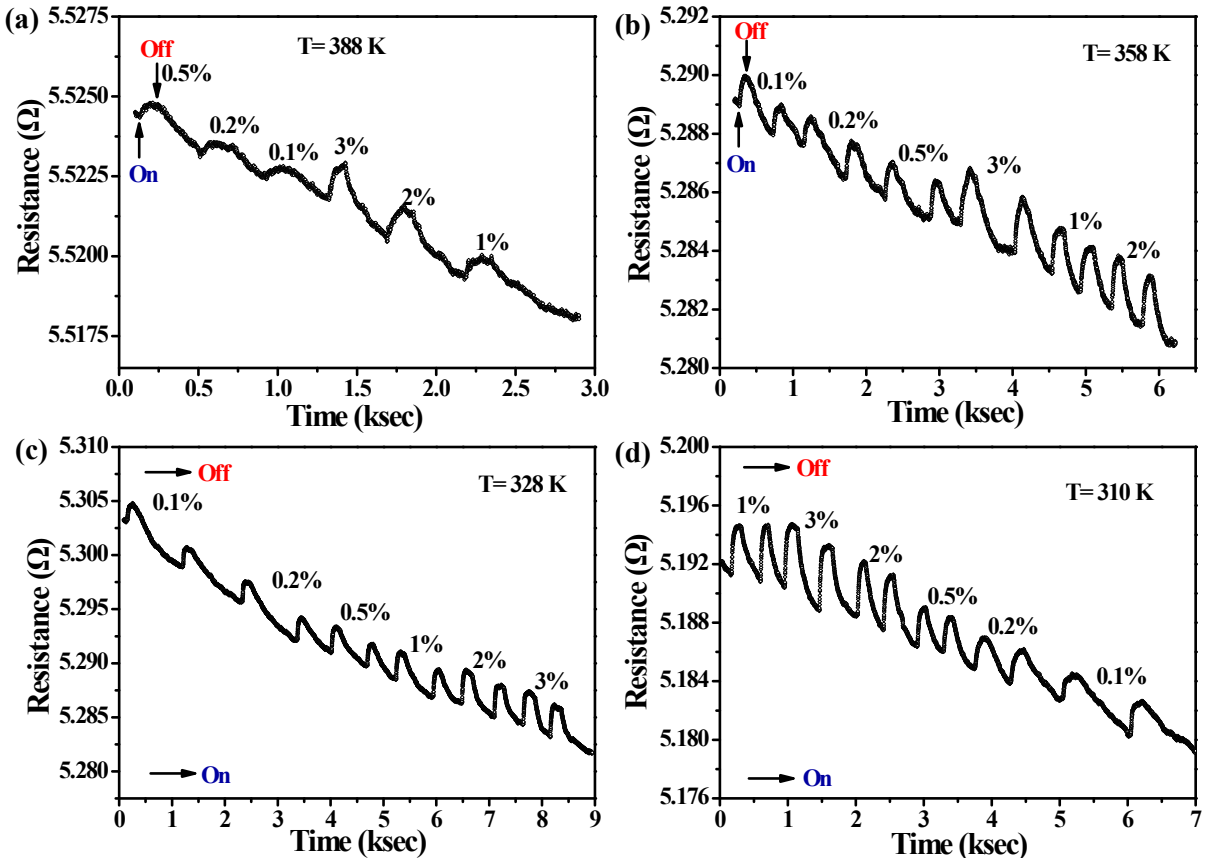

Figure S12-1. The transient response curves of the $Pd_{63}Co_{37}$ NWs sensor towards various H_2 concentrations at (a) 388 K, (b) 358 K, (c) 328 K and (d) 310 K, respectively.

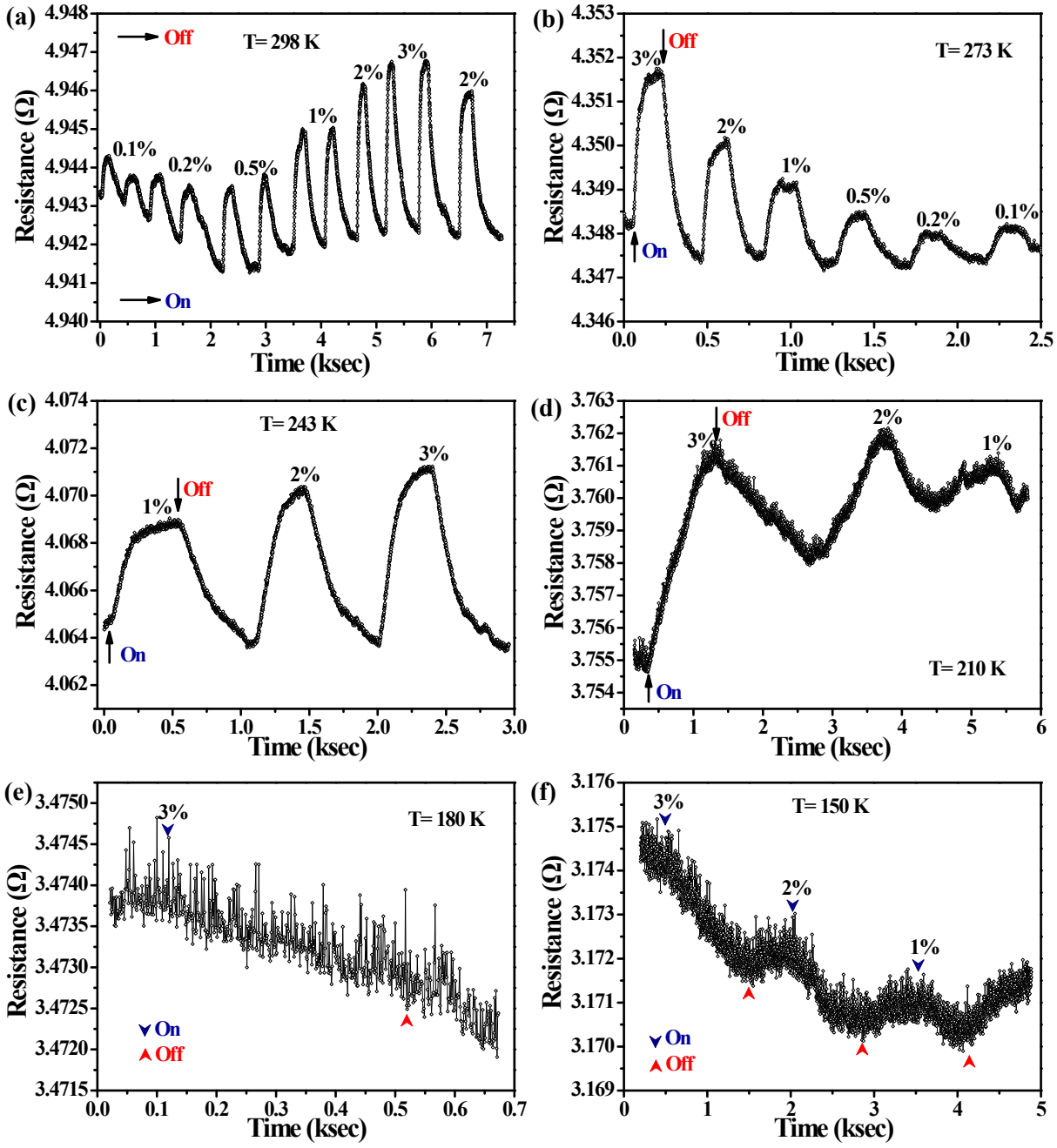

Figure S12-2. The transient response curves of the $Pd_{63}Co_{37}$ NWs sensor towards various H_2 concentrations at (a) 298 K, (b) 273 K, (c) 243 K, (d) 210 K, (e) 180 K and (f) 150 K, respectively.

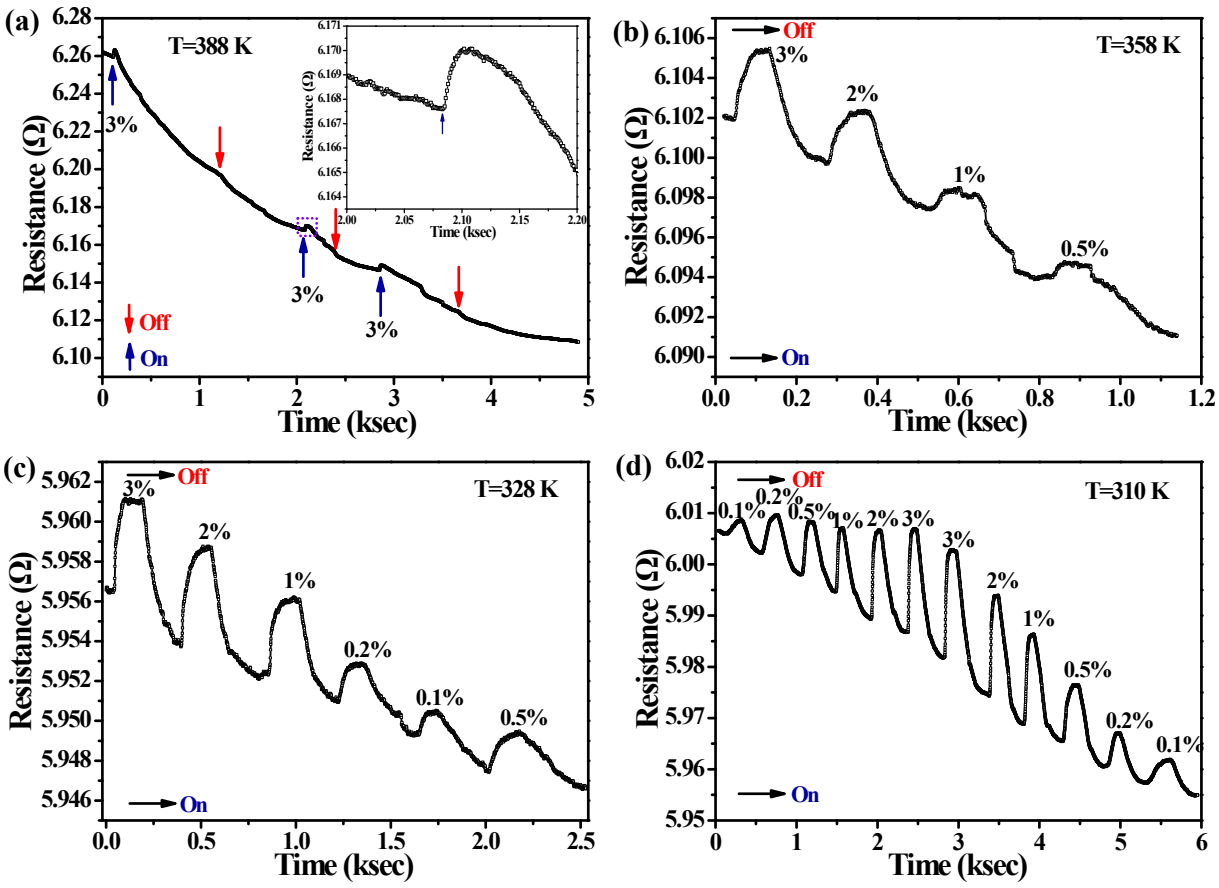

Figure S13-1. The transient response curves of the $Pd_{33}Co_{67}$ NWs sensor towards various H_2 concentrations at (a) 388 K, (b) 358 K, (c) 328 K and (d) 310 K, respectively.

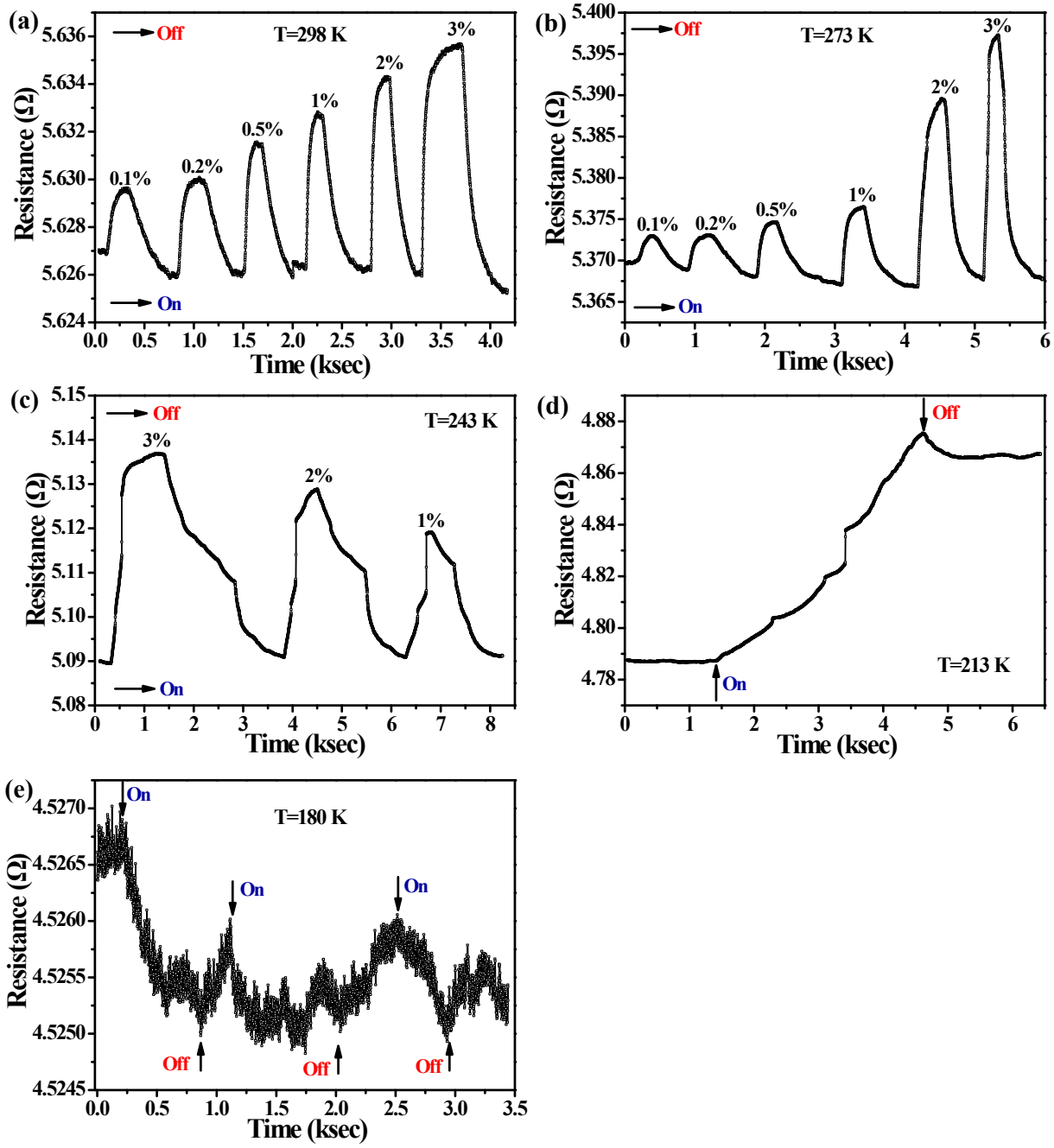

Figure S13-2. The transient response curves of the $Pd_{33}Co_{67}$ NWs sensor towards various H_2 concentrations at (a) 298 K, (b) 273 K, (c) 243 K, (d) 213 K and (e) 180 K, respectively.

References

1 D. Yang and L. F. Fonseca, *Nano lett.*, 2013, **13**, 5642-5646.

2 D. Yang, J. Carpena-Nunez, L. F. Fonseca, A. Biaggi-Labiosa and G. W. Hunter, *Sci. Rep.*, 2014, **4**, 3773.

3 L. Du, L. Zheng, H. Wei, S. Zheng, Z. Zhu, J. Chen and D. Yang, *ACS Appl. Nano Mater.*, 2019, **2**, 1178-1184.

4 D. Yang, G. Meng, C. Zhu and X. Zhu, *Chem. Commun.*, 2009, 7110-7112.